This article was downloaded by:
Publisher: KKG Publications
Registered office: 8, Jalan Kenanga SD 9/7 Bandar Sri Damansara, 52200 Malaysia

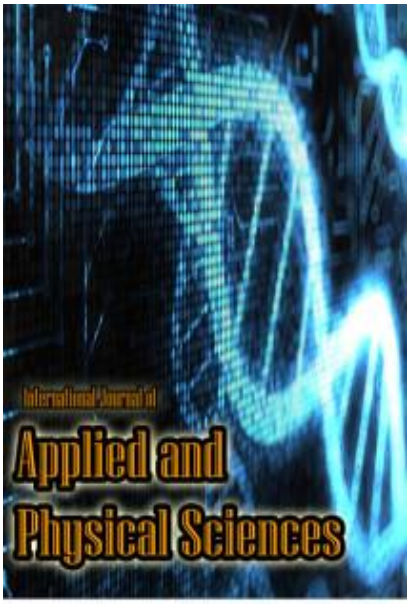

Key Knowledge Generation
Publication details, including instructions for authors and subscription information:
http://kkgpublications.com/applied-sciences/

Multi-State Phenomena and Hysteresis of Counterflow Flame over Tsuji Burner

Hsing-Sheng Chai[1], Vong-Ren Chen[2]

[1] General Education CenterAletheia University New Taipei City,Taiwan, R.O.C,
[2] AU Optronics Corporation Taichung, Taiwan, R.O.C

Published online: 21 June 2015

To cite this article: H. S. Chai and V. R. Chen. 2015, "Multi-State phenomena and hysteresis of counterflow flame over tsuji burner," *International Journal of Applied and Physical Sciences*, Vol. 1, no. 1, pp. 1-13.
DOI: https://dx.doi.org/10.20469/ijaps.50001
To link to this article: http://kkgpublications.com/wp-content/uploads/2015/12/IJAPS-50001.pdf

PLEASE SCROLL DOWN FOR ARTICLE

KKG Publications makes every effort to ascertain the precision of all the information (the "Content") contained in the publications on our platform. However, KKG Publications, our agents, and our licensors make no representations or warranties whatsoever as to the accuracy, completeness, or suitability for any purpose of the content. All opinions and views stated in this publication are not endorsed by KKG Publications. These are purely the opinions and views of authors. The accuracy of the content should not be relied upon and primary sources of information should be considered for any verification. KKG Publications shall not be liable for any costs, expenses, proceedings, loss, actions, demands, damages, expenses and other liabilities directly or indirectly caused in connection with given content.

This article may be utilized for research, edifying, and private study purposes. Any substantial or systematic reproduction, redistribution, reselling, loan, sub-licensing, systematic supply, or distribution in any form to anyone is expressly verboten.

KKG PUBLICATIONS

International Journal of Applied and Physical Sciences

IJAPS

2015, 1(1): 1-13

MULTI-STATE PHENOMENA AND HYSTERESIS OF COUNTERFLOW FLAME OVER TSUJI BURNER

HSING-SHENG CHAI[1*], VONG-REN CHEN[2]

[1]General Education CenterAletheia University New Taipei City, Taiwan, R.O.C,
[2]AU Optronics Corporation Taichung, Taiwan, R.O.C

Keywords:

Hysteresis
Blowoff
Tsuji Burner
Counter Flow Flame

Received: 4 March 2015
Accepted: 18 May 2015
Published: 21 June 2015

Abstract. This investigation focuses on flame hysteresis in a porous cylindrical burner. Different operating procedures of the experiment cause this hysteresis. Gradually increasing inflow velocity can transform the envelope flame into a wake flame. The blowoff curve is plotted by determining every critical inflow velocity that makes an envelope flame become a wake flame at various fuel-ejection velocities. In contrast, reducing the inflow velocity can transform the wake or lift-off flame into an envelope one. The reattachment curve can be obtained by the same method to explore the blowoff curve, but the intake process is reversed. However, these two curves are not coincident, except at the origin. The discrepancy between them is called hysteresis, and it results from the difference between the burning velocities associated with both curves. No hysteresis exists between two curves at the lowest fuel-ejection velocity because the difference between burning velocities is almost zero there. Then, raising the fuel-ejection velocity enhances hysteresis and the discrepancy between the two curves. However, when the fuel-ejection velocity exceeds a critical value, the intensity of hysteresis remains almost invariant and causes the two curves to parallel to each other.

© 2015 KKG Publications. All rights reserved.

INTRODUCTION

This is an experimental investigation of the multi-state phenomena of a counter flow flame in a porous cylindrical burner, the so-called Tsuji burner. This work extends that of [1]. It is motivated by a series of studies by [2] and employs an experimental set-up that is similar to that used by [1] displayed in Figure 1, to investigate the possible existence of the dual phenomena of a counter flow flame, and determine their mechanisms.

[3, 4] and [5] conducted a series of experiments on the counter flow diffusion flame in the forward stagnation region of a porous cylinder. These researchers considered in detail the corresponding extinction limits and aerodynamic effects, as well as the temperature and the stable-species-concentration fields of this flame. They identified two flame extinction limits. Blowoff, caused by a large velocity gradient (flame stretch), occurs because of chemical limits on the
rate of combustion in the flame zone. Substantial heat losses cause thermal quenching at a low fuel-ejection velocity. However, they reported no hysteresis.

[1] conducted the experimental visualization of a counter flow diffusion flame in a porous cylinder. Flame configurations and transition processes were elucidated using an image, photograph taken at nighttime settings, that's the night shot function. The parameters of the experiment were the inflow velocity and fuel-ejection velocity, respectively, with two fuel-ejection areas - half fuel-ejection area (S=180°) and full-ejection area (S=360°). At the half fuel-ejection area (S=180°), they found that the stand-off distance fell and flame length increased as the inflow velocity increased because of a greater flame stretch when the fuel-ejection velocity was fixed. As inflow velocity increased, the envelope, wake, side, lift-off and late wake flames appeared in order. However, for full-ejection area (S=360°) with a fixed high fuel-ejection velocity, the envelope flame directly transformed into a lift-off flame without the appearance of a wake flame as the inflow velocity increased. The major feature of the experiment was the occurrence of a lift-off flame.

[6] numerical study explored the counter flow flame in a porous cylinder. They employed two-dimensional complete Navier-Stokes momentum, energy and species equations with one-step finite-rate chemical kinetics. Their parametric studies were based on the Damkohler number (Da), a function of inflow velocity, and the dimensionless fuel-ejection velocity. As Da declined, the envelope, side, and wake flames appeared in order. However, reducing the dimension fuel-ejection velocity caused the envelope flame directly to become a wake flame, such that no side flame was formed. Also, when a limiting flow velocity was reached, the flame was extinguished completely, and hysteresis was not studied. [7] modified the original combustion model used

*Corresponding author: Hsing-Sheng Chai
E-mail: au4289@mail.au.edu.tw

Content from this work is copyrighted by KKG Publications, which permits restricted commercial use, distribution and reproduction in any medium under a written permission. Users may print articles for educational and research uses only, provided the original author and source are credited. Any further utilization of this work *must* maintain attribution to the author(s), the title of the work and journal citation in the form of a proper scientific referencing.

innumerical study to adopt four-step chemical kinetics rather than one–step overall kinetics. The parametric study was based on variations in inflow velocity (Uin) and fuel-ejection area (S). The most interesting feature predicted by this numerical study is the existence of a lift-off flame, which was not observed [6].

[2] applied the canonical laws of droplets to simulate the multiplicities states and inter-phase exchange rates during the ignition of droplets. They found that the irreversible processes, related to transition from an envelope flame to a wake flame, are the major mechanism of the transition duality. However, the transition duality herein forms a hysteresis loop, characterized a series of state variations over burning droplets. When the Reynolds number is between the higher (ReE) and the lower (ReR) value, the flame may be configured as either an envelope flame or a wake flame, by increasing or reducing the Reynolds number, whereas the flame configuration of the droplet is only an envelope flame as the Reynolds number is less than ReR. When the Reynolds number exceeds ReE, only a wake configuration exists. Accordingly, they defined these phenomena together as transition duality due to the existence of multiple states at a fixed Reynolds number, and were documented in another study [8] later.

[9] experimentally examined the methane flame transition in a stagnation-point flow. They found that a multi-solution can only arise in a lean fuel concentration in a stagnation-point flow upon a decrease or increase in the concentration of methane. Namely, under given conditions of fixed fuel concentration, inflow velocity and stagnation height, the methane flames appear at two positions in the Bunsen jet. At low methane concentration, the flame configuration can change between flat flame and cone flame. However, without interference, the flame configuration and the variation of the height of the Bunsen jet are quite different during the decrease or increase in methane concentration.

[10] experimentally studied the stability of flames at the nozzle port by altering the gas velocity. They found that when the gas velocity increases at a given butane concentration, the flame moves from a position that is close to the port to one that is far from it, and then the flame near the port is transformed into a lifted flame. Then, the lifted flame can be drawn back to the port by reducing the gas velocity below the lift-off velocity. The lift–off velocity at each fuel concentration will yield a lift curve. The transition velocity curve, transformed from a lift flame into a flame near the port, will become a drop-back curve. However, between the lift and drop-back curves, multi-states may exist in the lifted flame or the flame at the port.

This work elucidates the duality and hysteresis phenomena by varying the inflow velocities (Uin) from high to low at a fixed fuel-ejection velocity (Vw) in a circular cylindrical burner. This burner blows pure methane from its front half side, the surface that faces the intake flow. The rear half side of the porous burner is coated to prevent fuel ejection. Accordingly, the fuel is completely ejected from the front 180° central angle surface, and this case (front half side fuel-ejection) is designated as S=180°. Also, the unfinished work of [1] will be completed, which is the portion that fuel-ejection velocity exceeds 2.8 cm/s during an increase in the inflow velocity. The variable parameter is the inflow velocity (Uin) at each specified fuel-ejection velocity (Vw) under the front half fuel-ejection area (S=180°).

Experimental Apparatus

The experimental setup comprises a wind tunnel and a porous sintered cylindrical burner. Figure 1 depicts the entire experimental setup. The apparatus are described as follows.

Wind Tunnel

The wind tunnel is designed to provide a laminar, uniform oxidizer flow to the porous cylindrical burner, from the surface of which the fuel is ejected. It is open-circuit and orientated vertically upwards. Most of the design concepts of such a wind tunnel are from NIST [11].

The inlet velocity of the test section is determined using the AMCA 210-85 standard nozzle-method [12]: the volume flow rate is determined and used to deduce the flow velocity. The error in AMCA 210-85 is within 3% when the velocity is between 0.21 m/s and 3.3 m/s, but raises to 5% when the velocity is below 0.21 m/s.

The following procedure is adopted to confirm the uniformity and stability of the flow velocity in the test section. At the rim of the test-section entrance are four holes through which sensors are plugged into the flow to verify its uniformity (Figure 2). The sensors are hot wires. If the velocities at various positions are almost equal, then it can be certain that the flow is uniform and stable ahead of the burner, as displayed in Figure 3.

Porous Sintered Cylindrical Burner

The porous cylindrical burner is comprised of inner and outer parts. The diameter of the inner part is 20±0.5 mm, and that of outer part is 30±0.5 mm. The outer part is a replaceable piece of porous sintered stainless steel, with 20-μm pores and a length of 40±0.5 mm. The inner part is a cylindrical brass rod with internal water-cooling and fuel supply grooves. The outer part is screwed onto the inner part. The cooling device consists of a water tank, pump, cooler and connected piping.

The fuel is 99.99% methane (CH4), and its flow rate is controlled and measured using a digital mass flow controller (MC-2100ENC, Lintec) with a high-performance microprocessor. The fuel-ejection velocity is determined by dividing the fuel volume flow rate by the available fuel-ejection area over the surface of the burner.

Visualization System

A digital video (DCR-TRV50, SONY) is applied to visualize and record the flame profiles, such as the envelope, wake, and lift-off flames. A special night-shot function is used to record various

KKG PUBLICATIONS

flames in a dark laboratory environment. All images, recorded on a cassette tape, are transmitted to a PC for processing and analysis using Corel VideoStudio X2 software. The pixel intensities are adopted to present graphically the flame structures, in Spotlight 1.0 software.

Uncertainty Analysis

An uncertainty analysis is carried out here to estimate the uncertainty levels in the experiment. Formulae for evaluating the uncertainties in the experiment can be found in numerous investigations [13, 14] and textbooks [15, 16]. Table 1 summarizes the results of the uncertainty analysis.

Experimental Repeatability

To verify the accuracy and confidence in the results of the experiment, the procedures of changing the inflow velocities for each fuel-ejection velocity were executed three times to ensure the experimental repeatability. In this preliminary measurement, the transition velocity was a critical value to investigate the flame behaviors as the incoming velocity diminished. The reattachment curves reveal the transition velocities. Flame transformation is a function of fuel-ejection velocity. It recorded three measured data and made an averaged value for each fuel-ejection velocity. The averaged values were plotted as a dashed curve. Table 2 presents the three measured data, their averaged value, and the error for blowoff and reattachment curves. The error is defined as the ratio of the absolute difference between the maximum and minimum values of the three data to their averaged value. The errors are generally within an acceptable range (the maximum is less than 8.82%) and the repeatability is moderately excellent. Figure 4 is a graphical representation of Table 2. In the following section, we will discuss in detail the flame transition processes. Figure 5 in the following section demonstrates that the hysteresis phenomenon is characterized based on a continuation of Chen et al.'s experiment [1].

RESULTS AND DISCUSSION

This investigation elucidates variation in flame structure by varying the inflow velocity (Uin) from high to low at a fixed fuel-ejection velocity (Vw) for a forward half porous cylinder (S=180o). Whether the hysteresis phenomena of the flame structures occur as the inflow velocity is changed from the initial value to the critical value, and then back to the initial value, is determined.

In a previous study [1] experimentally visualized the counterflow diffusion flame in a porous cylinder as they raised the inflow velocity from an initial value to the critical one. They identified the flame transition velocity from an envelope flame to a wake flame at each specified fuel-ejection velocity and obtained a blowoff curve. Now, the reverse process, defined as a drop back process by reducing the inflow velocity from the critical value to a low one, is performed here. The incoming air velocity falls from 1.87 m/s to 0.389 m/s, and the fuel-ejection velocity ranges from 0.78 cm/s to 5.6 cm/s. Figure 5 shows plots of the experimental results with those of [1]; each point represents a measured datum and the dashed lines represent average values. The dashed curve, called the reattachment curve, differs significantly from the blowoff curve. The two curves are not coincident except at the origin. This feature is termed as duality phenomenon. When the fuel-ejection velocity is below 0.78 cm/s at an initial inflow velocity of 0.389 m/s, the flame becomes unstable and cannot exist because of wall quenching. However, increasing the fuel-ejection velocity causes the reattachment curve, to have the shape of a meniscus with an inflection point at Vw= 1.4 cm/s. However, the curve continues to rise as the fuel-ejection velocity increases to 5.6 cm/s on the right hand side of the inflection point. Due to the limitation of digital mass flow controller, the fuel-ejection velocity cannot be reached above the value of 5.6 cm/s.

Reducing the inflow velocity from 1.87 m/s to 0.389 m/s in the same region yields a sequence of flame pattern variations, which are displayed in Figs. 6, 7, and 8, in which the ejection velocities are fixed at Vw = 4.592 cm/s, Vw = 3.696 cm/s, and Vw = 2.69 cm/s, respectively. These figures identify the three types of flame in this region. They are wake flame, lift-off flame, and envelope flame. Initially, a wake flame occurs close to the rear surface of the porous cylinder. As the inflow velocity declines slightly, it vanishes and transforms into a lift-off flame. As the inflow velocity continues to decline to a particular value, the lift-off flame vanishes and its two flame fronts directly emerge in front of the porous cylinder to form an envelope flame. This phenomenon is a flash-back, which is caused by a balance position between the burning velocity to the inflow velocity. A comparison among these figures reveals that the transition velocity, at which a lift-off flame is transformed into an envelope flame, slightly increases with the fuel-ejection velocity, because more fuel is carried downstream to form a mixture that is closer to the stoichiometric ratio as the fuel-ejection velocity increases. Hence, such a mixture causes flash-back to occur early, as expected. As the burning velocity of flame front exceeds the inflow velocity, the envelope flame appears in the front stagnation region of the porous cylinder immediately after the lift-off flame disappears from the rear of the porous cylinder. At the reflection point, the fuel-ejection velocity equals 1.4 cm/s, and the corresponding flame patterns are displayed in Figure 9. This figure demonstrates that this has a great effect on the burning velocity of the wake flame in the rear of the cylinder because of the wall quenching effect. This effect causes a reduction in the reaction rate since heat is lost to the surface of the cylinder. Accordingly, the quenching effect markedly reduces the burning velocity of the wake flame, and can further delay the transformation of a wake flame into an envelope flame until the inflow velocity falls to a certain value below the burning velocity of the wake flame. However, in the reattachment curve on the left hand side of the inflection point, a wake flame transforms directly into an envelope flame in this region as the

inflow velocity decreases. Figure 10 indicates that the transition velocity in this region exceeds that at the reflection point because the boundary layer effect strongly influences the inflow velocity and burning velocity, causing the inflow velocity in the boundary layer to be less than the burning velocity. Therefore, it leads to a higher transition velocity at the left of the reflection point.

Hysteresis appears in numerous nonlinear systems that involve irreversible processes. The state of such a system is determined by the operating environment and initial status of the system. Comparing the reattachment curve with the blowoff curve conducted by [1] the discrepancy between these two curves is termed as hysteresis. The hysteresis phenomena arise from the difference between the burning velocities associated with both curves. Therefore, through hysteresis phenomena, it also points out several important findings. At the lowest fuel ejection velocity, no hysteresis exists between the blowoff and reattachment curves because the burning velocities at Vw = 0.78 cm/s are almost equal. Accordingly, the two curves intersect with each other to form a node at the lowest value, at which no hysteresis exists. Then, as the fuel-ejection velocity increases, it enhances the hysteresis and the discrepancy between the blowoff and reattachment curve increases. Hysteresis at a fuel-ejection velocity of Vw = 3.3 cm/s clearly exceeds that at the low fuel-ejection velocity. As the fuel-ejection velocity exceeds this critical value, the intensity of the hysteresis effect remains almost constant and causes the blowoff curve to be parallel to the reattachment curve, because the excess fuel is carried to the rear of the porous cylinder and mixes with air to form a flammable mixture as the fuel-ejection velocity is large, enhancing the burning velocity associated with transformation from wake or lift-off flame to envelope flame. However, it suppresses the combustion rate of flame transition from the envelope flame to the wake flame. Hence, the blowoff curve is parallel to the reattachment curve when the fuel-ejection velocity exceeds 3.3 cm/s.

CONCLUSION

This investigation extends the experimental work performed by [1] reversing the operating process by reducing the incoming velocity from a high value to its original value, rather than increasing the inflow velocity, and making more thorough measurements to catch the flame hysteresis in a porous cylindrical burner. The parameters of interest are the inflow velocity (Uin) and fuel-ejection velocity (Vw). This study emphasizes the mechanism of hysteresis, which was unidentified by [1] but observed in the droplet combustion researches of [2, 8].

Most of the design concepts for the present used wind tunnel are taken from NIST [11]. The burner is made of porous sintered stainless steel, with 20-μm pores and a length of 40±0.5 mm. The fuel is 99.99% methane. The inlet velocity of the test section is determined using the AMCA 210-85 standard nozzle-method [12]. At the rim of the test-section entrance are four holes, through them hot wires are plugged into the flow to confirm its uniformity.

In a parametric study, the inflow velocity declines from 1.87 m/s to 0.389 m/s, and the fuel-ejection velocity ranges from 0.78 cm/s to 5.6 cm/s. The corresponding results yield a reattachment curve that differs greatly from the blowoff curve that was obtained by [12]. The two curves both reveal the critical flame transition velocity and the corresponding fuel-ejection velocity, but the difference between them is the intake process. The reattachment curve is obtained by reducing the inflow velocity from high to low. In contrast, the blowoff curve is obtained by increasing the inflow velocity from low to high. Thus, the two operating procedures are completely reversed. However, the curves are not coincident except at the origin. This feature is called duality phenomenon. The discrepancy between these two curves is called hysteresis. The hysteresis phenomena results from the difference between the burning velocities of both curves. At the lowest fuel-ejection velocity, no hysteresis exists between the blowoff and reattachment curves because the burning velocities of both curves are almost equal over there. Then, as the fuel-ejection velocity increases, the hysteresis is enhanced, increasing the discrepancy between the blowoff and reattachment curves. However, as the fuel-ejection velocity rises above a critical value, the intensity of the hysteresis effect almost remains constant and causes the blowoff curve parallel to the reattachment curve. Consequently, the reattachment curve has the shape of a meniscus with an inflection point at Vw= 1.4 cm/s.

REFERENCES

[1] D. Chen, C. Chang, and C. Chen "Experimental visualizations of counter flow flame behind porous cylinder," *Journal of the Chinese Society of Mechanical Engineers,* vol. 27, no. 3, pp. 321-334 2006.

[2] H.H. Chiu, and J. S. Huang "Multiple-State phenomena and hysteresis of a combusting isolated droplet," *Atomization Spray.*, vol. 6, no. 1, 1996.

[3] H. Tsuji, and I. Yamaoka, "The counterflow diffusion flame in the forward stagnation region of a porous cylinder," in *Symp. (International) on Combustion,* vol. 11, no. 1, 1967, pp. 979-984.

[4] H. Tsuji and I. Yamaoka, "Structure analysis of counterflow diffusion flames in the forward stagnation region of a porous cylinder," in *Symp. (International) on Combustion,* Vol. 13, no.1, 19971, pp. 723-731.

KKG PUBLICATIONS

[5] H. Tsuji, "Counterflow diffusion flames," in *Progress in Energy and Combustion Science*, vol. 8, no. 2, pp. 93-119, 1982.

[6] C. H. Chen, and F. B. Weng "Flame stabilization and blowoff over a porous cylinder," *Combust. Sci. Technol.*, vol. 73, no. 1-3, pp. 427-446 1990.

[7] S. S. Tsa, and Chen, C. H. (2003). Flame stabilization over a Tsuji burner by four-step chemical reaction," *Combust. Sci. Technol.*, Vol. 175, no. 11, pp. 2061-2093.

[8] J. S. Huang, and H. H. Chiu "Multistate behavior of a droplet in dilute sprays," *Atomization and Sprays*, vol. 7, no. 5, pp. 479-506 1997.

[9] W. D. Hsieh, and T. H. Lin. "Multi-Solution and dynamic transition of methane flames in a stagnation-point flow," *in Proc. of the 13th Conference Combustion Institute of Republic of China, 2003.*

[10] K. Wohl, N. M. Kapp, and C. Gazley, "The stability of open flames, " In *Symp. on Combustion and Flame, and Explosion Phenomena*, vol. 3, no. 1, pp. 3-21, 1949.

[11] J. C. Yang, M. K. Donnelly, N. C. Prive, and W. L. Grosshandler, "Dispersed liquid agent fire suppression screen apparatus, NISTIR 6319," National Institute of Standards and Technology.

[12] A. S. H. R. A. E. Standard, "*Laboratory Methods of Testing Fans for Rating,"* US: American Society of Heating, Refrigerating and Air-Conditioning Engineers, 1985.

[13] H. Tsuji and I. Yamaoka, "The structure of counterflow diffusion flames in the forward stagnation region of a porous cylinder," in *Symp. (International) on Combustion*, 1969, vol. 12, no. 1, pp. 997-1005.

[14] R. J. Moffat, "Contributions to the theory of single-sample uncertainty analysis", *ASME, Transactions, Journal of Fluids Engineering*, vol. 104, no. 2, 250-58 1982.

[15] R. W. Fox, A. T. McDonald, and P. J. Pritchard, " *Introduction to Fluid Mechanics,"* vol. 7, 1985 :New York: John Wiley & Sons.

[16] J. P. Holman. *Experimental Methods for Engineers* (5th ed.). McGraw-Hill, New York, 1989.

TABLE 1
Summary of Uncertainty Analyses

Parameters	Uncertainty
D_i , D_o, L_B , a , b	±0.5 mm
A	±1.267%
A_{Burner}	±2.084%
N	±0.09%
ρ_{air}	±0.201%
$\dot{V}_0$	±2.2%
Q_{fuel}	±1%
U_{in}	±2.54%
V_w	±2.31%
Re	±3.04%

KKG PUBLICATIONS

Table 2
Experimental Repeatability

Fuel-ejection velocity (cm/s)	Transition velocity (1st measured) (m/s)	Transition velocity (2nd measured) (m/s)	Transition velocity (3rd measured) (m/s)	Average value of three times (m/s)	Error (%)
0.78	0.49	0.5	0.48	0.49	4.08
0.9	0.476	0.468	0.468	0.471	1.69
1.01	0.46	0.452	0.46	0.457	1.75
1.12	0.41	0.426	0.407	0.414	4.59
1.23	0.43	0.408	0.417	0.418	5.26
1.34	0.41	0.408	0.426	0.415	4.34
1.4	0.41	0.408	0.417	0.412	2.18
1.46	0.41	0.408	0.426	0.415	4.34
1.57	0.41	0.408	0.417	0.412	2.18
1.68	0.39	0.408	0.426	0.408	8.82
1.79	0.41	0.408	0.426	0.415	4.34
1.9	0.39	0.408	0.426	0.408	8.82
2.02	0.41	0.426	0.435	0.424	5.9
2.13	0.44	0.426	0.443	0.436	3.9
2.24	0.41	0.429	0.443	0.427	7.73
2.35	0.41	0.431	0.443	0.428	7.71
2.46	0.43	0.435	0.45	0.438	4.56
2.58	0.43	0.444	0.459	0.444	6.53
2.69	0.444	0.444	0.46	0.449	3.56
2.8	0.444	0.447	0.457	0.449	2.9
2.91	0.452	0.455	0.468	0.458	3.5
3.02	0.46	0.457	0.473	0.463	3.5
3.14	0.47	0.46	0.475	0.468	3.2
3.25	0.472	0.46	0.468	0.467	2.57
3.36	0.492	0.465	0.472	0.476	5.67
3.472	0.485	0.46	0.476	0.474	5.27
3.584	0.492	0.468	0.468	0.476	5.04
3.696	0.495	0.476	0.475	0.482	4.15
3.808	0.504	0.476	0.476	0.485	5.77
3.92	0.5	0.478	0.476	0.485	4.94
4.032	0.492	0.481	0.48	0.484	2.48
4.144	0.492	0.484	0.484	0.487	1.64
4.368	0.495	0.492	0.492	0.493	0.6
4.592	0.495	0.492	0.49	0.492	1.01
4.816	0.5	0.498	0.492	0.497	1.6
5.152	0.51	0.507	0.504	0.507	1.18
5.6	0.53	0.515	0.507	0.517	4.4

KKG PUBLICATIONS

FIGURE 1
Overall Experimental System

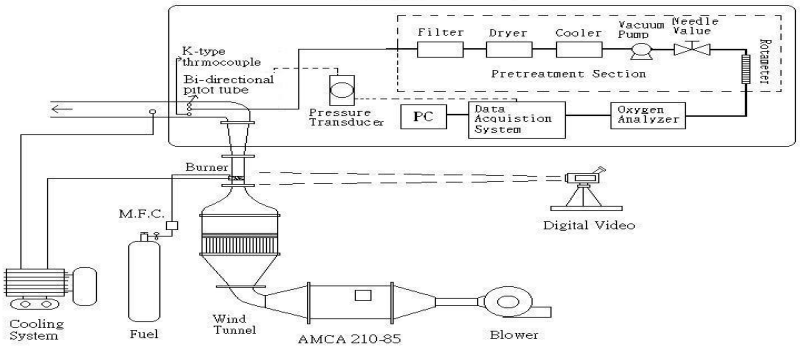

Figure 2
Positions of hot wires

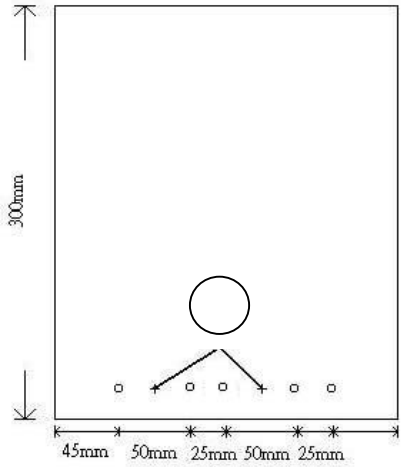

Figure 3
Inflow Velocity at each Position in the Test Section

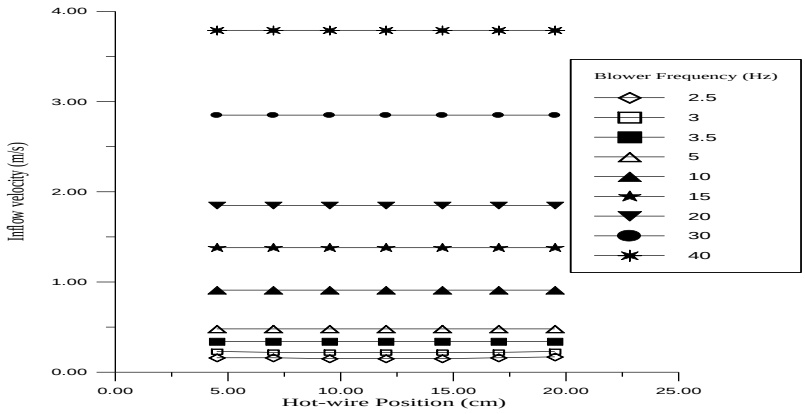

FIGURE 4
Errors Associated with Experimental Repeatability

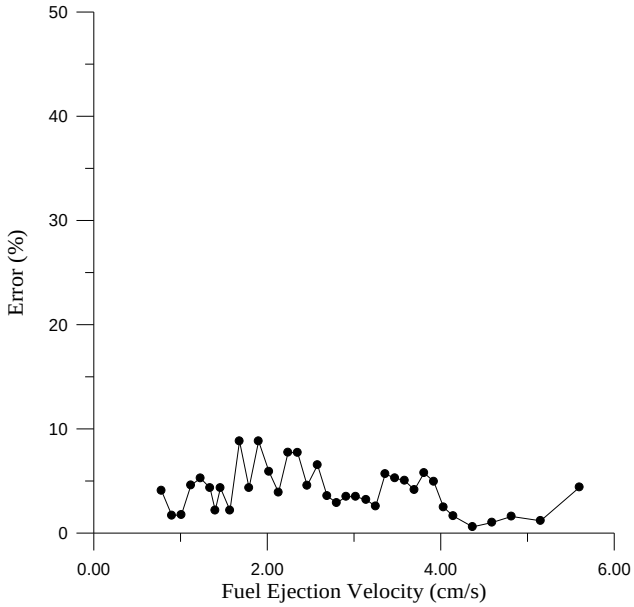

Figure 5
Reattachment and Blowoff Curves

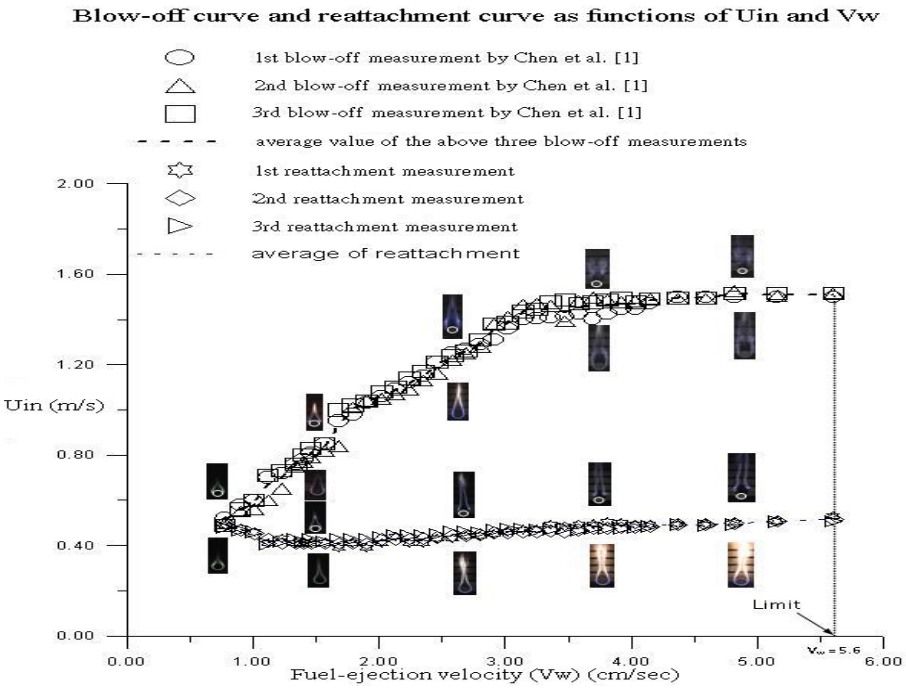

KKG PUBLICATIONS

FIGURE 6

Series Of Flame Configurations For Various Inflow Velocities (Vw = 4.592 cm/s, S=180。): (a) Uin = 1.85 m/s (b) Uin = 1.09 m/s (c) Uin = 0.53 m/s and (d) Uin = 0.495 m/s

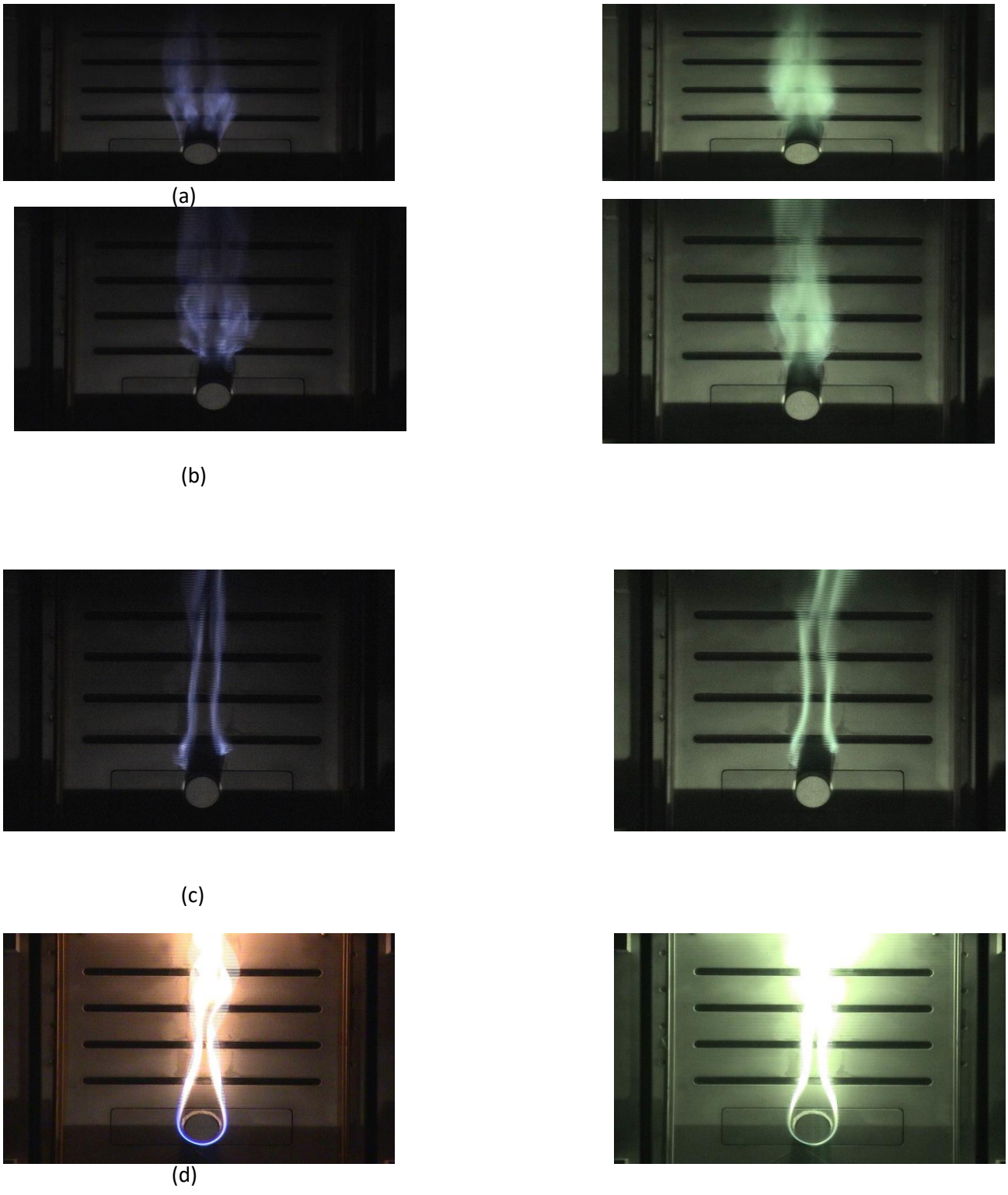

(a)

(b)

(c)

(d)

KKG PUBLICATIONS

FIGURE 7

Series of Flame Configurations for Various Inflow Velocities (V_w = 3.696 cm/s, S=180°): (a) U_{in} = 1.85 m/s (b) U_{in} = 0.696 m/s (c) U_{in} = 0.5 m/s and (d) U_{in} = 0.475 m/s

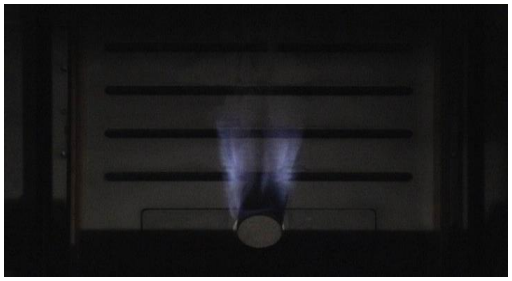

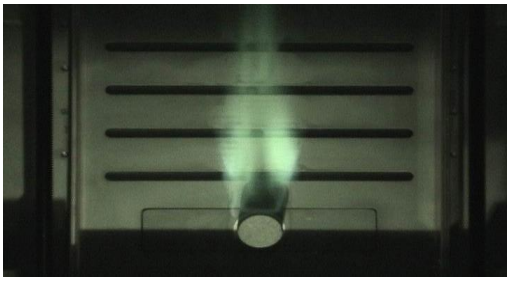

(a)

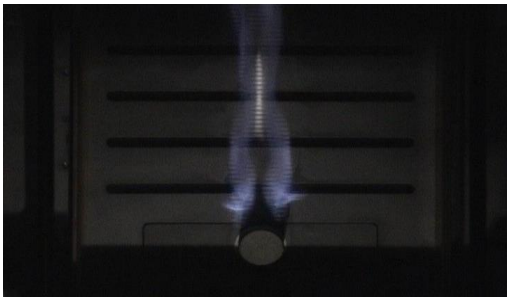

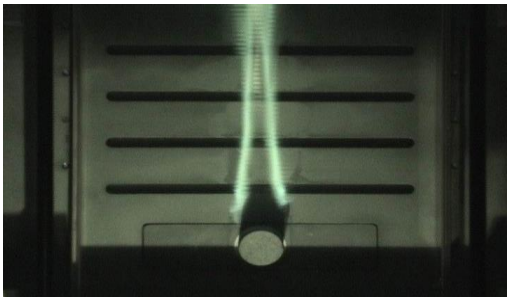

(b)

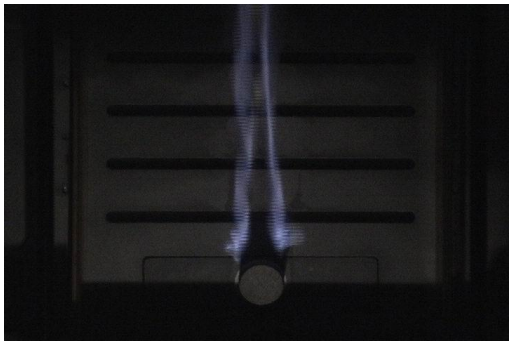

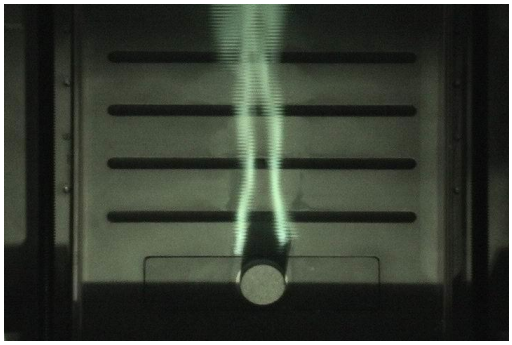

(c)

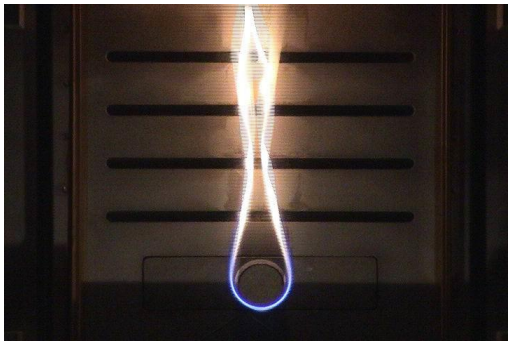

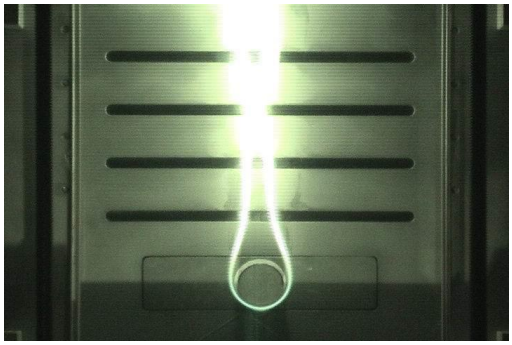

FIGURE 8

Series of Flame Configurations for Various Inflow Velocities (Vw = 2.69 cm/s, S=180。): (a) Uin = 1.86 m/s (b) Uin = 0.55 m/s (c) Uin = 0.46 m/s and (d) Uin = 0.44 m/s

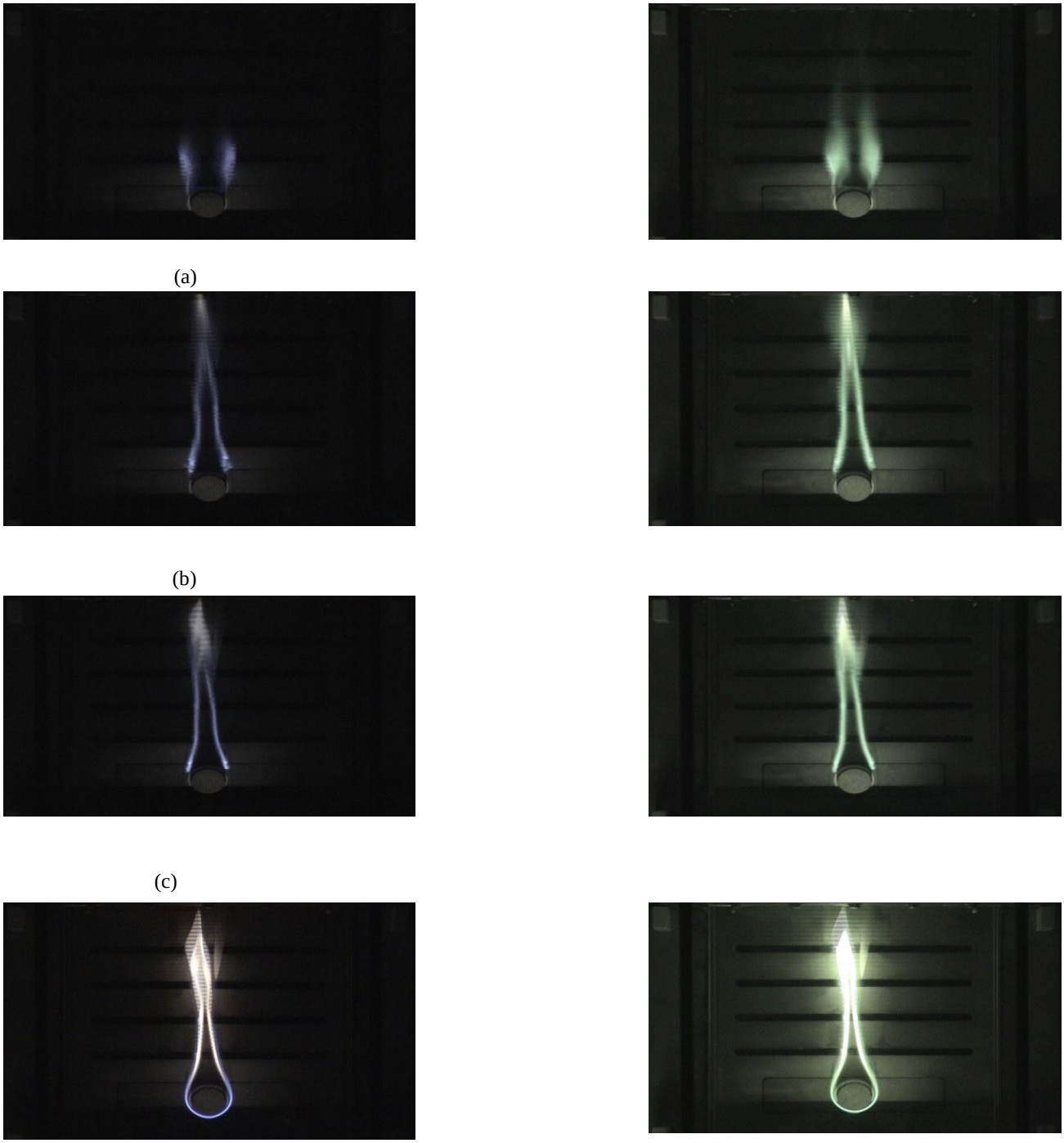

(a)

(b)

(c)

(d)

KKG PUBLICATIONS

FIGURE 9

Series of Flame Configurations for Various Inflow Velocities (Vw = 1.4 cm/s, S=180。): (a) Uin = 1.86 m/s (b) Uin = 0.55 m/s (c) Uin = 0.426 m/s and (d) Uin = 0.41 m/s

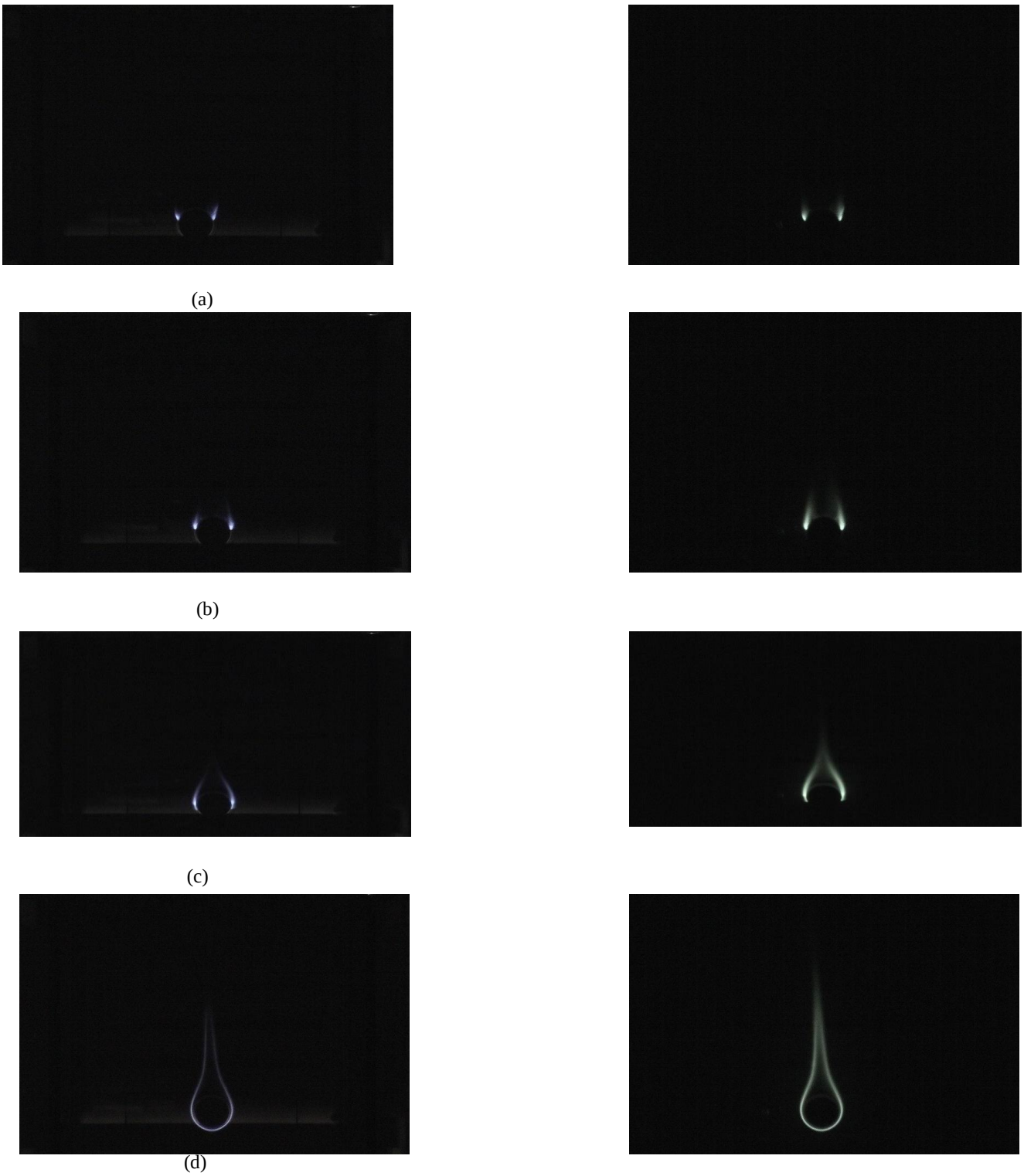

(a)

(b)

(c)

(d)

KKG PUBLICATIONS

FIGURE 10

Series of Flame Configurations for Various Inflow Velocities (Vw = 0.9 cm/s, S=180。): (a) Uin = 1.86 m/s (b) Uin = 0.9 m/s (c) Uin = 0.5 m/s and (d) Uin = 0.48 m/s

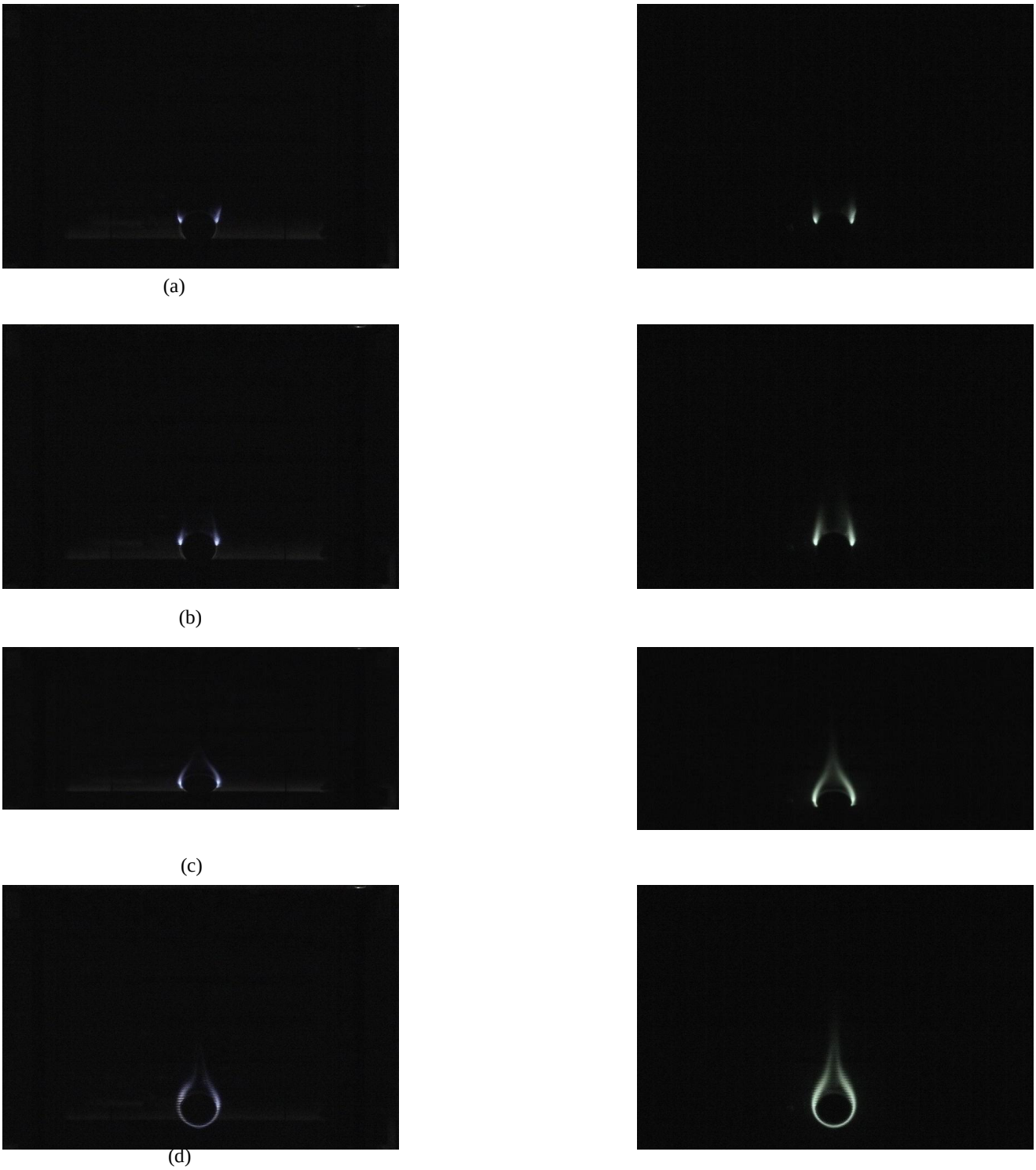

(a)

(b)

(c)

(d)